Int J Adv Manuf Technol (2016) 82:163–177
DOI 10.1007/s00170-015-7359-9

ORIGINAL ARTICLE

Analytical and experimental analysis of the formability of copper-stainless-steel 304L clad metal sheets in deep drawing

Farshid Dehghani[1] · **Mahmoud Salimi**[1]

Received: 23 January 2015 / Accepted: 20 May 2015 / Published online: 9 June 2015

Abstract The formability of the clad metal sheets is influenced by many factors such as mechanical properties of the component metals, so that producing clad cups with high formability free of defects is not easily possible. The behavior of clad sheet, vis-à-vis single-layer sheets, is comprehensively studied through experimental as well as numerical methods using the finite element analysis. In this study, the limiting draw ratio and thickness variations of copper-stainless-steel 304L clad metal sheet have been investigated. Finite element simulations were conducted to study the process and to predict the fracture position. The experimental results in various conditions were compared and the desirable state was recognized. Results illustrated that the thickness distribution of stronger material (stainless-steel 304L) was somewhat more uniform than the weaker one (copper layer). It is demonstrated that the strain distributions in the deep-drawn cups obtained by the FE method can be used to predict the location of fracture in the experimental tests. Furthermore, it was found that the formability of clad sheets, in different layout settings, with respect to various parameters, followed the same trends as single-layer sheets.

Keywords Clad metal sheet · Deep drawing · Finite element analysis (FEA) · Formability

✉ Farshid Dehghani
Dehghani.mechanic@yahoo.com

Mahmoud Salimi
salimi@cc.iut.ac.ir

[1] Department of Mechanical Engineering, Isfahan University of Technology, Isfahan 8415683111, Iran

1 Introduction

Composite materials have been widely used in modern industries such as electrical industries, automotive, and cooking apparatus [1–3]. One way to achieve the desired mechanical and physical properties is to bond different metals as clad sheets. Each layer of the clad sheet may have different mechanical, chemical, and physical properties; therefore, such properties as high-yield strength, high-elastic-plastic strain, resistance to fracture, electrical conductivity, and corrosion resistance, not available in a single metal, can be achieved by bonding different metals together as clad sheets. Some clad sheets are designed to suit different internal and external environments. For instance, when the bi-metal connections of expansion valve are produced from copper stainless-steel 304L-clad sheet, the materials of the interior and the exterior are chosen to be copper and stainless-steel 304L respectively, as the thermal conductivity of the stainless-steel is lower than that of copper; the energy loss of the expansion valves is decreased.

Clad sheets are produced by different methods such as cold-rolled welding, hot-rolled welding, and explosive welding. To remove the residual stress, resulting from bonding process, suitable heat treatment of the clad sheet is performed [4]. In heat treatment of clad sheets, the bonded sheets are heat-treated with low temperatures in long duration creating metallurgical bond at the interface. This would release the residual stress, fortify the bonding strength (to resist rupturing of layers at the interface during the forming process), and increase the formability [4–6].

In the production line, clad sheets are sheared, bent, hydroformed and deep-drawn to produce clad metal parts. Deep drawing is one of the well-known metal forming processes available to manufacturers. In deep drawing, the workpiece usually is controlled by a blank holder and pulled into the matrix by a punch until the required form is achieved. Numerous attempts have been made to investigate the

formability of deep drawing process for single-layer sheets [7–14]; however, only few studies have probed into the formability of clad sheets manufactured by roll and explosive welding, in spite of their widespread applications.

Rees and Power [15] studied the formability of the zinc-steel-clad sheets. Using the forming limit diagrams (FLDs), they demonstrated that formability depended on the strain paths. Hino et al. [16] investigated the draw ratio of aluminum-stainless-steel-clad sheets. Their results showed that the draw ratio increased when the punch was in contact with the stronger layer. Habibi Parsa et al. [17] studied the redrawing of aluminum-stainless-steel-clad sheets experimentally and analytically using the finite element (FE) simulation. They evaluated thickness influence and setting conditions for each layer and illustrated that the maximum formability occurred for a thickness ratio of about one to three for aluminum and stainless-steel layers respectively. Yoshida and Hino [18] investigated the forming limit of stainless-steel-clad aluminum sheets under plane stress condition. Their analytical analysis and experimental observations demonstrated that the FLDs of the laminates lie between those of their component metals. Tseng et al. [19] analyzed the formability of aluminum-copper clad sheets in relation to the thickness of each layer and blank holder pressure. They concluded that the formability of clad sheets was influenced by the residual stresses developed due to cold-roll welding prior to drawing and reduced in comparison to each of the two single-layer materials. As for this history of research, suitable processes like post-heat treatment after cladding to obtain high formability for the clad metals were ignored.

The present study is targeted at investigating the effect of various parameters on axial symmetrical deep drawing process using a circular-clad sheet. Deep drawing of clad metal sheets of copper stainless-steel is performed after bonding the sheets by explosive welding and heat treatment processes. Die components are designed and manufactured to suit the forming process and finally the influences of material properties and experimental setups on draw ratio, thickness distribution, forming stresses, and fracture position of drawn cups are analyzed.

2 Mechanical properties of clad sheet and its component materials

2.1 Materials and cladding method

In this study, the explosive welding method was used to bond copper and stainless-steel 304L sheets. Each sheet has a primary thickness of one millimeter. The chemical compounds of the sheets have been tabulated in Table 1. In order to achieve a uniform thickness, cold-rolling process, investigated by the authors in their previous paper [4], was used. The thickness of the clad metal sheets in the cold-rolling process was reduced by approximately 5 % so that the final thickness of each layer was about 0.95 mm (schematic views of explosive welding and cold rolling are given in Fig. 1a, b).

2.2 Heat treatment

In clad sheets, anisotropy of the sheets, the bond direction in the joining process and the heat treatment operation [20] are effective factors in forming, location, and the height of earing at different orientations in deep drawing process. Thus, to avoid alterations in the material property, the bond of the sheets in explosive welding and the direction of cold rolling were chosen to be the same direction as that of the primary rolling of each layer. To create the metallurgical bond between the two layers, enhance the formability, and relieve the residual stress, the sheets were kept at a temperature of about 300 °C for about 32 h (Fig. 1c) as established by the authors in their previous publications [4].

2.3 Tensile test

With the aim of probing the deformation of each layer during the forming process, the properties of the materials were analyzed separately. Copper and stainless-steel 304L sheets underwent thickness reduction of about 5 % with initial thickness of one millimeter each, in the same direction as the primary rolling of the sheets. Afterwards, each layer was heat-treated in the same condition as the clad sheets. After preparing the samples in accordance with the *ASTM-E8M04* standard, uniaxial tension tests in four different directions 0, 45, 90, and 135° were carried out, Fig. 1d. The average of the true stress-strain characteristics were derived according to the relation: $\overline{\sigma} = (\sigma_0 + \sigma_{45} + \sigma_{90} + \sigma_{135})/4$. This test was performed by a *Zwick/Roell Z400 UTM* Machine, at an initial strain rate of 5 mm/min. The materials properties for each metal sheet and clad sheet after cold rolling and heat treatment as well as the materials properties for

Table 1 The chemical composition of stainless-steel 304L and copper

Elements (wt.%)	Cr	Ni	Mn	C	Si	S	Al	Cu	Fe
AISI 304L	18.91	8.44	1.79	0.015	0.483	0.03	–	0.043	Balanced
Copper	0.03	0.03	–	–	–	–	0.155	Balanced	0.05

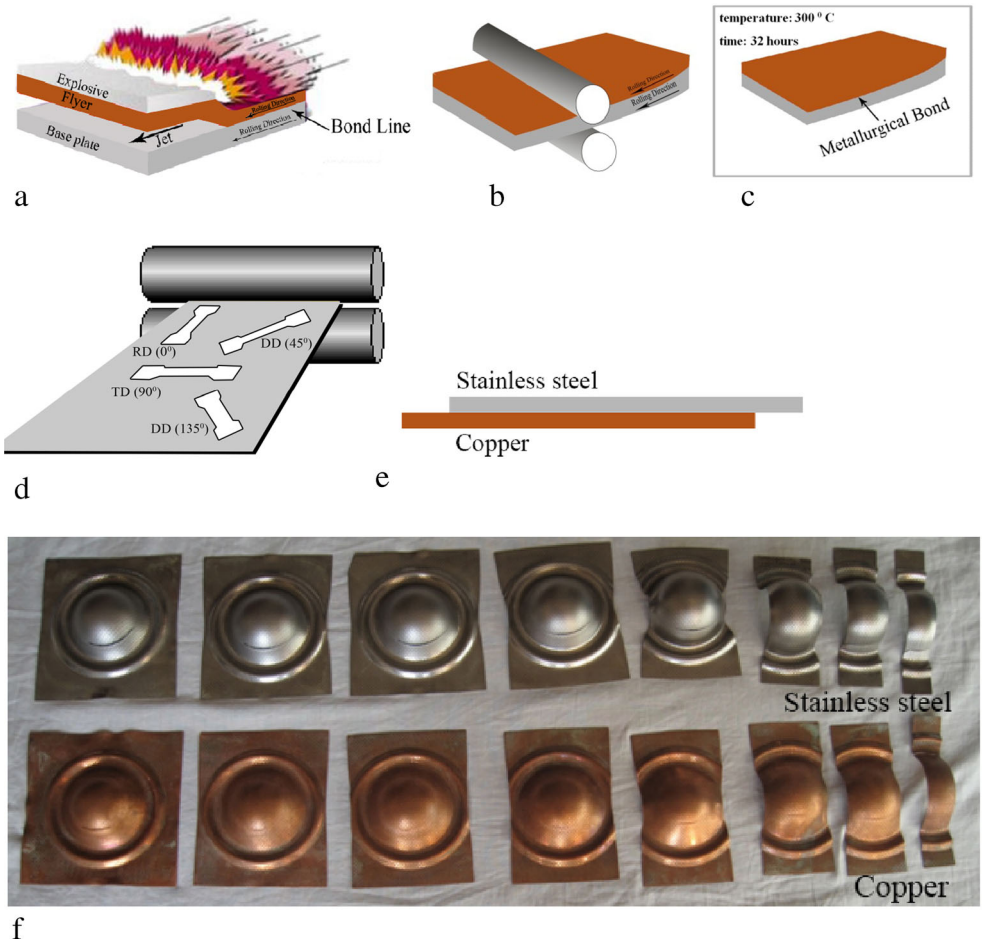

Fig. 1 Schematic of **a** explosive welding process, **b** cold-rolled welding, **c** post heat- treatment, **d** uniaxial tension test specimen directions, **e** peeling test sample, and **f** selected samples of stainless-steel and copper after forming limit tests

single-layer sheets as raw materials are given in Tables 2 and 3, respectively.

Considering isotropic work-hardening Swift law, the flow stress can be calculated as follows:

$$\sigma = K(\varepsilon_0 + \bar{\varepsilon}^p)^n \quad (1)$$

In this relation, σ is the equivalent stress, $\bar{\varepsilon}^p$ is the equivalent plastic strain, K is the material constant, n is the strain-hardening exponent and $\varepsilon_0=(Y_0/K)^{1/n}$ is the strain at yield point where Y_0 is the yield stress.

2.4 Peeling test

In order to assess the joint quality and the possibility of presence of imperfections at the interface, after post-heat treatment, a peeling test was performed according to ASTM-D903-93 standard. Figure 1e shows the peeling test sample. This test was conducted using a *Zwick/Roell Z400 UTM* Machine with a constant crosshead speed of 2 mm/min. In this test the work dissipated in peeling is calculated according to the following equation:

$$\mathrm{Up} = \frac{FX}{W} \quad (2)$$

In this relation, F, X, and W are the mean peeling force, the amount of crosshead movement, and the width of sample respectively.

The results indicated that at the initial steps of the process, after 2 mm of punch travel, the clad sheet was ruptured from the copper part. The maximum force of

Table 2 Material properties of single-layer sheets and clad sheet after cold rolling and heat treatment

Material	R_0	$R_{45–135}$ (DD)		R_{90} (TD)	S_y (MPa)	S_{ut} (MPa)	K (MPa)	n
Stainless-steel	0.979	1.425	1.475	0.922	347	1247	1479	0.506
Copper	0.394	0.702	0.783	0.598	79	329	458.6	0.527
Clad sheet	0.766	1.461		1.247	519.8	868	1105.9	0.289

Table 3 Material properties of raw single-layer sheets

Material	R_0 (RD)	R_{45} (DD)	R_{90} (TD)	S_y (MPa)	S_{ut} (MPa)	K (MPa)	n
Stainless-steel	1.215	1.327	1.24	298	1235	1484	0.553
Copper	0.763	0.767	0.762	78	393	469.4	0.331

peeling enhanced the ultimate tensile strength of the copper layer, to about 329 MPa. This means that the created bond at the interface was stronger than that of the copper material. As a result, in the numerical modeling, the deformation behavior of the copper stainless-steel-clad metal sheets was assumed to be equivalent to a clad sheet of different mechanical characteristics where no slip between layers is occurred.

2.5 Forming limit test

The formability of clad sheets is influenced by different parameters such as the plastic strains at each layer, the thickness ratio, etc. During the forming process, it is possible for a layer to reach its critical strain and rupture. To determine the FLDs for each layer, the stretch forming tests were carried out. The samples of copper and stainless-steel 304L steel sheets were prepared with the same cold-work history and heat treatment as those prepared for uniaxial tension test with 120 mm lengths and various widths from 12 to 120 mm with an increment of 12 mm. Afterwards, the sheet surface was electrochemically etched with circles of 0.1-in. diameters to measure the principal strains in the localized neck region. This test was performed by an Ericson Tool Machine 150/7025, using a semi-spherical punch of 60 mm diameter with a uniform velocity of 0.4 mm/s and maximum blank holder force of 110 and 25 KN for stainless-steel 304L and copper sheet respectively (Fig. 1f). Figures 2 and 3 depict the forming limit diagrams for stainless-steel 304L and copper sheet respectively. Since the direction of the greater and smaller elongations in the sheet plane coincide to that of the major and minor axes of developed ellipses, the strains in these directions and very close to the location of fracture of each specimen are recorded and termed the "major strain" and the "minor strain" respectively. The values of these strains are plotted against one another. The major strain is chosen to be the ordinate. Due to variations in thickness and mechanical properties of the sheet material, the friction at the interface of the tool and work-piece and the reading error in recording the strain some discrepancies may occur. The curve fitting to the strain points obtained by experiment, defines the forming limit diagram. The zone below the curve is known as the safe zone; the elements lying on the curve are in the necking zone while fracture occurs for the elements having the strains above the curve. For the finite element simulation, the engineering major and minor strains were converted to true major and minor strains.

3 Deep drawing

Deep drawing of circular cups is broadly used in various applications. Generally, multiple drawing is required to achieve the final deep-drawn cups. Thus, it is desirable to improve the formability of the material prior to the deep drawing process to minimize the number of drawings.

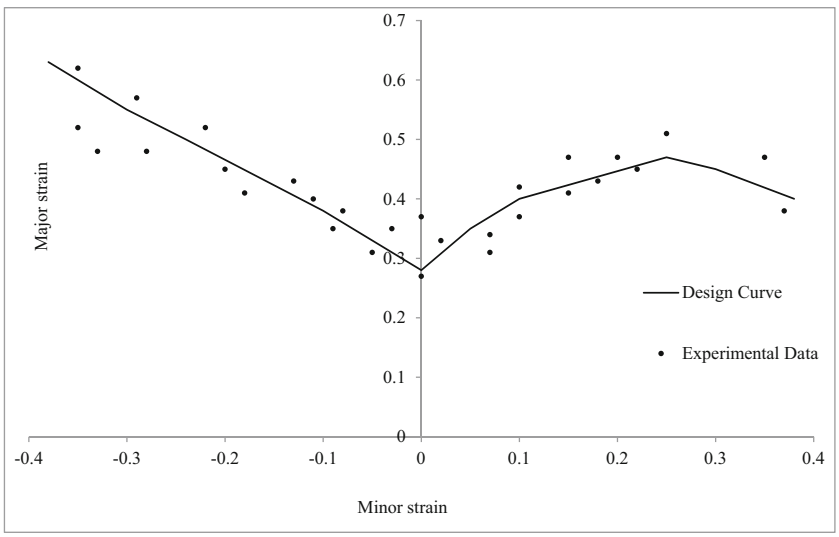

Fig. 2 Experimental FLD result of SUS 304L sheet after cold rolling and heat treatment

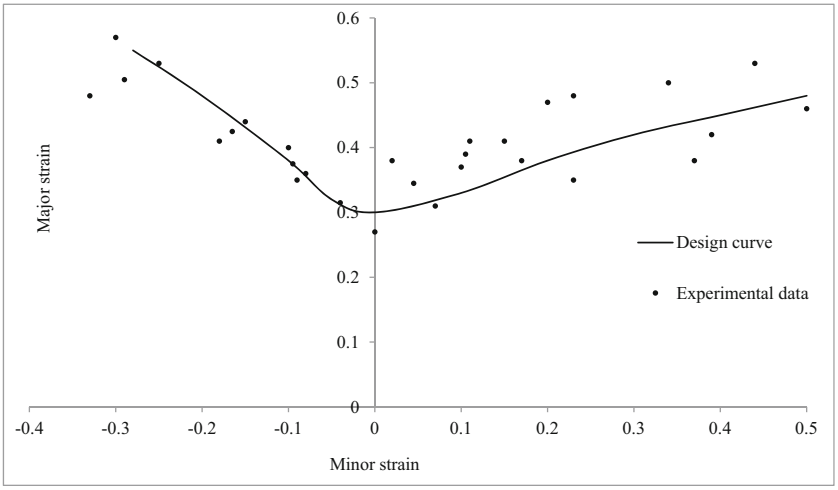

Fig. 3 Experimental FLD result of copper sheet after cold rolling and heat treatment

3.1 Limiting draw ratio

In deep drawing process, the limiting draw ratio (LDR) is defined as follows:

$$\beta = \frac{D_{\max}}{d_{\text{punch}}} \tag{3}$$

Where $D_{\max}$ is the maximum blank diameter and d_{punch} is the punch diameter. In the deep drawing process of clad sheets, the draw ratio is affected by material properties of the components metal. Using different thickness ratios and rolling directions for each layer, it is possible to produce clad sheets with different formability.

3.2 Thickness distribution

One of the desirable quality criteria for the deformed components is possessing uniform thickness distribution so that the thickness variations drop as low as possible. The plastic deformations for each layer of the clad sheet located inside or outside of the deformed cup depend on many parameters like the each layer strength that makes it a compound and complicated materials behavior.

The thickness on the work-piece was measured along the cup walls from center of the cup bottom to top of the cup at several locations with an interval of 5 mm using an optical microscope 50× and anvil micrometer having a least count of 0.01 mm, for clad and single-layer cups, respectively. Considering the marginal difference between ears and valleys in low-draw ratios, the thickness was only measured in rolling direction (RD), where copper located inside the cup and stainless-steel 304L at outside. For high-draw ratios, the thickness was measured in RD as well as diagonal direction (DD) at different layout setting.

3.3 Experimental work

To determine LDR, a flat-headed punch of 50 mm diameter was used. The circular samples in the range of 90 to 125 mm diameters, producing draw ratios of 1.8 to 2.5, were prepared and the experimental tests were performed using a hydraulic press of 160 ton.

In this study, the effective parameters were chosen to be die edge radius (r_d)=4, 5, 6, and 7t_0 [21], punch edge radius (r_p)= 4t_0 and 5t_0 [22], Blank holder pressure (BHP)=0.875, 4, 8, and 10 MPa [23], friction states: dry condition (no lubrication), application of oil at all contact surfaces except the punch surface, polyethylene (Pe) sheets in both sides of work-pieces and finally the compound of oil and polyethylene [22]. Moreover, to avoid ironing of drawn cup, the wall clearance was chosen to be 20 % of t_0.

Figure 4 depicts the variations of BHP with respect to the die movement during the tests. The BHP increases almost linearly until it reaches a maximum value; thereafter, it remains almost constant for about 30 % of the stroke and then at the end of the process it reduces smoothly.

Adjustments to the experimental conditions for the failed products during the process were made on BHP first, then on the lubrication states, and then on r_p, and finally on r_d so that the perfect products were produced. Moreover, the limiting draw ratio of the perfect products was obtained. Experimental tests were carried out in turn on the single-layer sheets and the clad sheets. To achieve more accurate results, three samples of the same dimensions were used in a similar condition and the mean values were considered.

3.4 FE simulation

The explicit FEA using Abaqus software was conducted to analyze the deformation of the deep drawing for a circular-

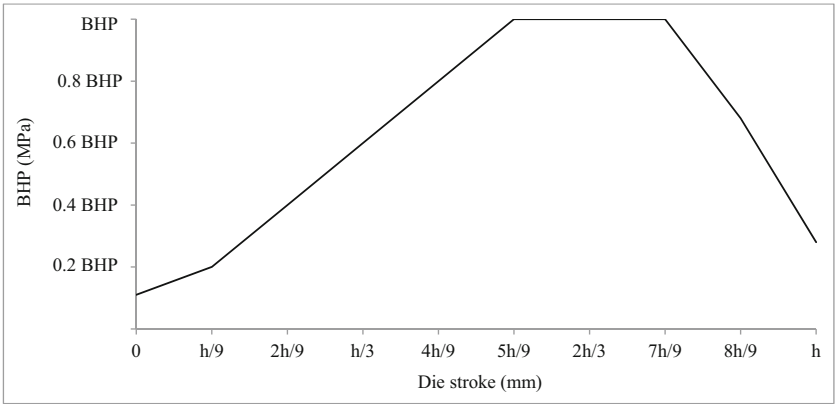

Fig. 4 Variations of BHP versus die stroke

clad blank. The copper-stainless-steel-clad blank was partitioned into two separate parts, bonded together at the interface with different mechanical properties. The materials characteristics obtained from the true stress-strain curve and the logarithm strains of the FLDs were defined separately for each part. The initial process parameters were selected from the experimental database. The punch, die, and blank holder were modeled as rigid. The punch was constrained fully and the die was slightly stroked down only along the *Z*-direction with a uniform velocity of 0.8 mm/s; simultaneously, the blank holder was moved with the same amount as the die. The penalty contact interfaces were utilized to model the contact between the clad metal sheet and the tools. The Coulomb coefficients of friction were assumed to be 0.05 for the contact areas between the die and blank surface and 0.15 for the other contact surfaces. The friction coefficients were intently chosen low to allow the effects of material anisotropy to control the process. BHP was exerted to the lower surface of the blank holder according to Fig. 4. To obtain the optimum number of elements for meshing the clad blanks, preliminary studies were conducted. It was found that there were 4810 elements in the radial direction and eight elements through thickness direction with reduced integration points. The four upper and four lower elements in the thickness direction were related to the stainless-steel and copper materials respectively. Two layers of the clad sheet were meshed by linear hexahedral elements of type C3D8R capable of tolerating high-strain and nonlinear behavior.

4 Results and discussions

The effects of different parameters on formability of the clad and the single-layer sheets are studied. Initially, the experimental test was carried out according to the primary values of: $r_d=r_p=4t_0$.

4.1 Effect of blank holder pressure

The BHP is one of the effective parameters on metal sheet formability. Wrinkle or fracture may occur if the BHP is set to be too low or too high.

The tests indicated that LDR for single and clad sheets was approximately the same and about 1.9. Setting of the BHP from 4 to 6 MPa and from 8 to 10 MPa created in turn thinning of the cup wall and failure since circumferential straining, due to higher blank holder pressure, is more constrained.

Figure 5 depicts the thickness strain distributions in stainless-steel 304L and the copper layers of the clad sheet for three different BHPs with no lubrication. The thickness distributions are divided into three distinct parts: the bottom, the arc portion, and the wall portion of the cup. At the bottom of the cup, where the distance of any point from the cup center is less than 20 mm, the thickness strain distributions are negligible. It is evident that the thinning occurs at the arc portion of the cup, 20–30 mm from the center of the cup. The thinnest portion is located at 25 mm away from the cup center. This is attributed to the maximum tensile force and this is the point where stress concentration takes place. The thickness of the cup wall is increased gradually from the lowest point to the top one, due to the compressive hoop stresses in the flange portion.

The average thickness distributions of each layer with respect to the variations of BHP of the clad sheet are given in Table 4. Figure 5 and also Table 4 illustrate that by reducing the BHP thinning is also decreased. According to Table 4 and experimental tests, it is concluded that excessive BHP does not only reduce the

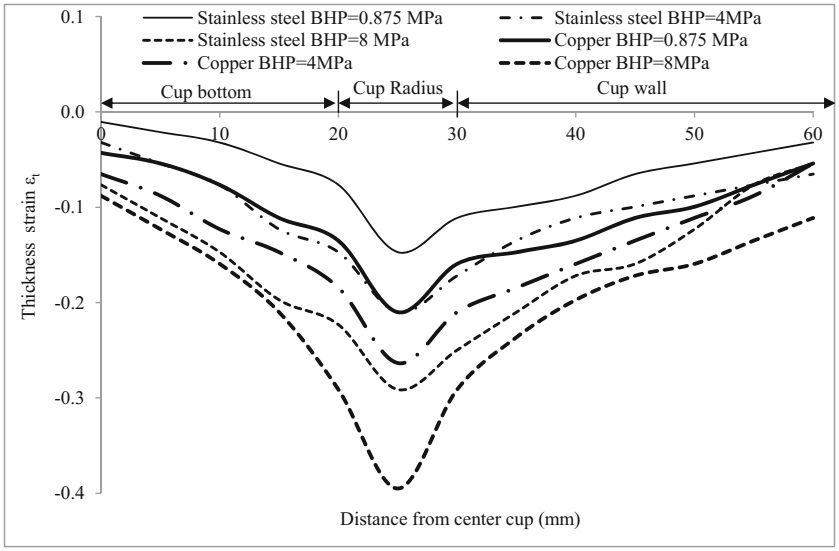

Fig. 5 Thickness strain distributions of SUS 304L and copper layers of drawn clad cup for different BHP, DR=1.9, r_d=r_p=4t_0, RD

component dimensional quality but also results in rapid abrasion of the die and increased production costs.

Comparison between thickness distributions in Fig. 5 reveals that decreasing in thickness of the copper layer, due to lower strength of this layer than the other layer, is higher while the reduction in thickness for the two layers is not uniform along the edge and cup wall.

Reducing the BHP from (8–10 MPa) to (6–8 MPa) to 0.875–4 MPa for a single-layer stainless-steel 304L and copper sheets increases the thickness of 8.42 %t_0 and 6.13 %t_0 at edges and 5.24 %t_0 and 4.64 %t_0 at the cup wall respectively, which is uniformly distributed. Furthermore, setting the BHP from 8 to 10 MPa for the single-layer causes the copper sheet to rupture. The results shed light on the fact that appropriate BHP for clad and single-layer sheets turns out to be from 0.875 to 4 MPa which was used in subsequent examinations.

Table 4 Average thickness at cup corner and wall

BHP (MPa)	Average thickness in the clad cup (mm) (initial thickness=0.95 mm)			
	Copper layer		Stainless-steel layer	
	Edge cup	Wall cup	Edge cup	Wall cup
0.875–4	0.8	0.86	0.85	0.89
4–8	0.76	0.84	0.8	0.86
8–10	0.69	0.8	0.74	0.83

4.2 Effect of lubrication

Lubrication is one of the important parameters affecting the quality and formability of sheet metals. Using appropriate lubricants can noticeably reduce friction and tool wear and provide a better material flow into the die cavity to achieve a better surface finish of the product.

To achieve draw ratios above 1.9, utilizing any lubricant such as oil, polyethylene, and oil and polyethylene is inevitable. By using appropriate lubricants, the LDR for single-layer stainless-steel 304L steel and clad sheet approached 2 and the LDR for single-layer copper achieved 2.1.

Figures 6 and 7 depict the influence of different friction states on thickness strain distributions in stainless-steel 304L and copper layers in clad sheet for a DR=1.9 respectively. It is axiomatic that simultaneous application of oil and polyethylene in comparison to dry condition makes the cup thickness to be more uniform as shown in these figures. Furthermore, simultaneous application of oil and polyethylene on thickness uniformity is more effective than the polyethylene/oil lubricant applied separately. The thickness distribution for polyethylene lubricant in comparison to the oil lubricant is approximately the same and the differences between the two cases are negligible.

The effect of lubrications on single-layer sheets is similar to clad sheets. Having considered the results, it is concluded that suitable lubricants for clad and single-layer sheets are simultaneous application of polyethylene and oil.

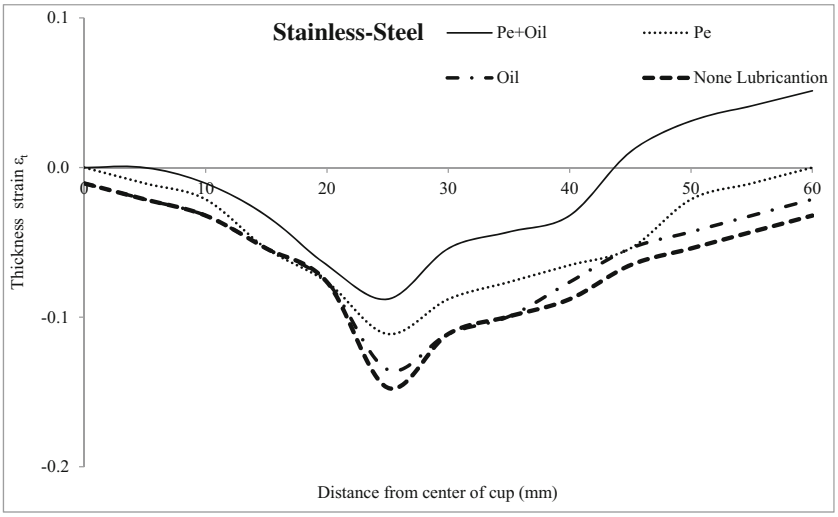

Fig. 6 Thickness strain distributions of SUS 304L layer of drawn clad cup for different friction states DR=1.9, r_d=r_p=4 t_0, BHP=0.875 MPa, RD

4.3 Effect of punch edge radius

The punch edge radius r_p controls the flow of blank material into the die cavity. Choosing an optimum value for r_p will increase the dimension of quality of the work-piece.

The experiments indicated that the punch edge radius had no effect on LDR.

Figure 8 depicts the effect of r_p on the thickness strain distributions of stainless-steel 304L and copper layers of the clad sheet for DR=1.9 respectively. Setting r_p=*5* t_0 in comparison to r_p=*4* t_0 results in a more uniform thickness at the cup corner.

The trend of increasing r_p from $4t_0$ to $5t_0$ for single-layer sheets is the same as the clad sheet. Considering these results, suitable r_p for clad and single-layer sheets was found to be $5t_0$ which was used for the subsequent tests.

4.4 Effect of die edge radius

The die edge radius r_d is one of the significant parameters affecting the process as it controls the metal flow into the die cavity. When r_d is too high, it leads to wrinkling within the cup wall while small die edge radius can result in tearing.

Referring to Table 5, it is evident that by increasing r_d the draw ratio is increased significantly from 2 to 2.3. The experimental results show that the optimum value for r_d in forming the clad cups is r_d=$5t_0$; in addition, increasing r_d, up to $5t_0$, has no effect on work-piece quality. Drawn cups free of fracture and wrinkle including the clad metals (in different layout settings) and single-layer sheets are represented in Fig. 9, with draw ratios from 1.8 to 2.4. The equal drawability of the single and clad sheets is mainly due to the fact that

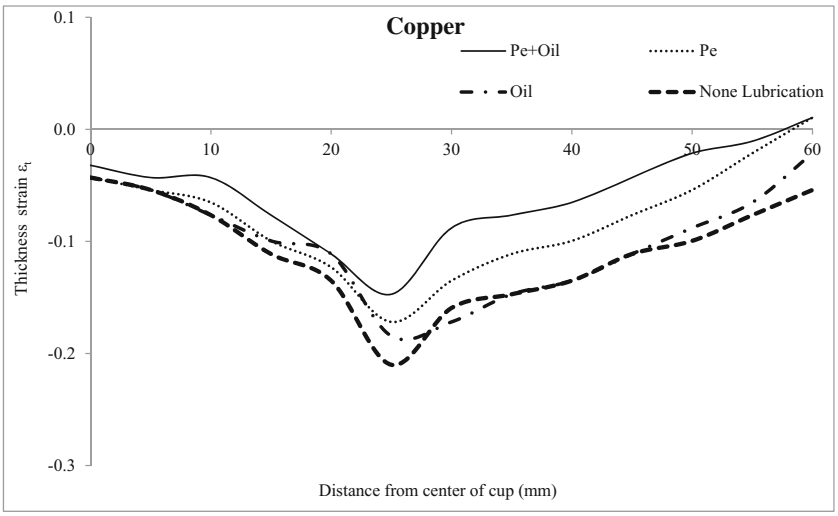

Fig. 7 Thickness strain distributions of copper layer of drawn clad cup for different friction states DR=1.9, r_d=r_p=4 t_0, BHP=0.875 MPa, RD

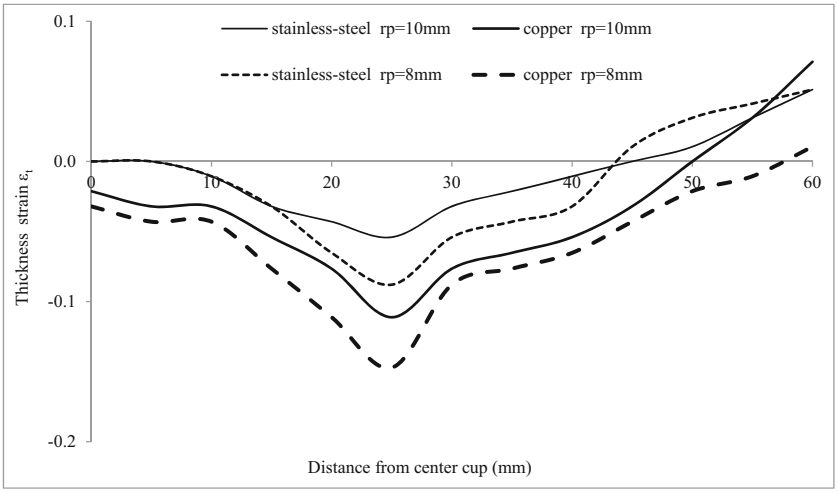

Fig. 8 Thickness strain distributions of SUS 304L and copper layers of drawn clad cup for different r_p, DR=1.9, $r_d=4t_0$, BHP=0.875 MPa, friction state= Oil+Pe, RD

they have approximately the same material properties, according to Tables 2 and 3.

Table 5 Effect of r_d

r_d (mm)	Lubrication	LDR	Description
10	Pe+Oil	1.8	Best result
10	Pe+Oil	1.9	Best result
10	None	2	Rupture
10	Oil	2	Satisfactory
10	Pe	2	Satisfactory
10	Pe+Oil	2	Best result
10	None	2.1	Rupture
10	Oil	2.1	Satisfactory
10	Pe	2.1	Satisfactory
10	Pe+Oil	2.1	Best result
10	Oil	2.2	Rupture
10	Pe	2.2	Satisfactory
10	Pe+Oil	2.2	Best result
10	Pe	2.3	Rupture
10	Pe+Oil	2.3	Best result
10	Pe+Oil	2.4	Rupture
12	Oil	2.2	Rupture
12	Pe	2.2	Satisfactory
12	Pe+Oil	2.2	Satisfactory
12	Pe	2.3	Rupture
12	Pe+Oil	2.3	Satisfactory
12	Pe+Oil	2.4	Rupture
14	Oil	2.2	Rupture
14	Pe	2.2	Satisfactory
14	Pe+Oil	2.2	Satisfactory
14	Pe	2.3	Rupture
14	Pe+Oil	2.3	Satisfactory
14	Pe+Oil	2.4	Rupture

Hino et al. [16], Habibi Parsa et al. [17], and Mori et al. [24] analyzed sheet-set condition on formability clad sheet aluminum-stainless-steel. In those papers, layout setting played an important role on the draw ratio on account of the fracture load changed in the forming process. Huang et al. [19] examined the formability of copper/Al clad sheet. Due to the fact that they ignored heat treatment process, low formability of the clad sheet was reported. Also, Takuda et al. [25, 26] and Yoshida et al. [18] proved that the formability of laminated composite sheet in order steel/Al and Al / stainless-steel 304 and /or 430 can be improved by different layout settings. However, in this study, since each single-layer materials had enough potential for plastic deformation for placement of very large strains, following post-heat treatment the mechanical properties of the two layers were not too far from single-layer sheets, so high-draw ratios equal to that of the single-layer sheets were obtained for the clad metal. This is achieved due to the proper post-heat treatment process and suitable choice of process parameters. With regard to these results, the relative location of the strong and the weak layers of the clad sheet had no effects on drawability.

Figure 10 depicts the effect of r_d on thickness strain distributions in stainless-steel 304L and copper layers of the clad sheet, for DR=2.3. Comparison between die edge radiuses illustrates that small r_d requires more energy for bending and unbending at the die corner and more drawing force and consequently the work-pieces may be ruptured. For large r_d, the radial drawing stress σ_r decreased and at the final drawing process the last portion of the sheet was formed freely (without BHP) leading to wrinkles and thickenings. Figure 11 demonstrates the distribution of forming stresses for different r_d in the numerical modeling. As it is seen, the average of forming stresses in $r_d=7t_0$ is lower than that of other values. As a result, the optimum r_d that can compromise the two phenomena, as mentioned above, is approximated to be: $r_d=5t_0$.

Increasing the die corner radius from $r_d=5t_0$ to $r_d=7t_0$ elevates the thickness at the wall top in turn to 4.57 $\%t_0$ and

Fig. 9 The products of clad and single-layer cups, DR=1.8–2.4

4.3 $\%t_0$ in the single-layer stainless-steel 304L sheets and single-layer copper sheets. Hence, the optimum value of r_d for clad and single-layer sheets is deduced to be $5t_0$.

Blank holder pressure augmentations, on the other hand, restrain materials flow by larger frictional forces resulting in a tendency to rupture in high-draw ratios. Figure 12a, b represents the manufactured cups, using different BHP and DR=2.3. From left to right, the figures illustrate single-layer copper cup, clad cup with external material stainless-steel 304L, and single-layer stainless-steel 304L cup. The BHP for exhibited samples in Fig. 12a is 0.875 to 4 MPa which is the safe range of the BHP for clad and single-layer cups. Setting the BHP of 4 to 8 MPa has the risk of rupture due to over thinning of the clad and single-layer cups. Figure 12b demonstrates the samples for BHP of 8 to 10 MPa where the clad and single-layer cups are ruptured. This incidence does not occur in lower draw ratios.

The results of high blank holder force in deep drawing composite sheet made by steel/brass [27] indicated that disbanding of layers during the forming process occurred. However, in the whole phases of this study the disbanding of layers did not happen mainly due to strong mechanical and metallurgical bands in the clad sheet.

4.5 The internal and external layers behavior

Studies on internal and external layers behavior are conducted in two different aspects; i.e., the thickness distributions and the forming stresses in different rolling directions. The drawn cups in both analyses have a DR=2.3, $r_d=r_p=5t_0$. Frictional state is considered to be a simultaneous application of oil and polyethylene while the BHP is set to be 0.875 MPa.

4.5.1 Comparison of the thickness distributions at the internal and external layers

The thickness distributions of the internal and external layers and single-layer cups in RD and DD with different layouts of setting layers are depicted in Figs. 13 and 14.

In Figs. 13 and 14, line *XY* represents the rolling directions of the clad cup. Due to the anisotropic nature of clad sheet, variations in the height of the cups are emerged when deep-drawn. In positions where materials flow faster, higher wall heights with lower thicknesses, known as ears, are produced. Valleys appear in positions where the cup walls are thicker and the heights are shorter due to the fact that a high *r* value gives high deformation resistance of blank; thus materials are blocked in this

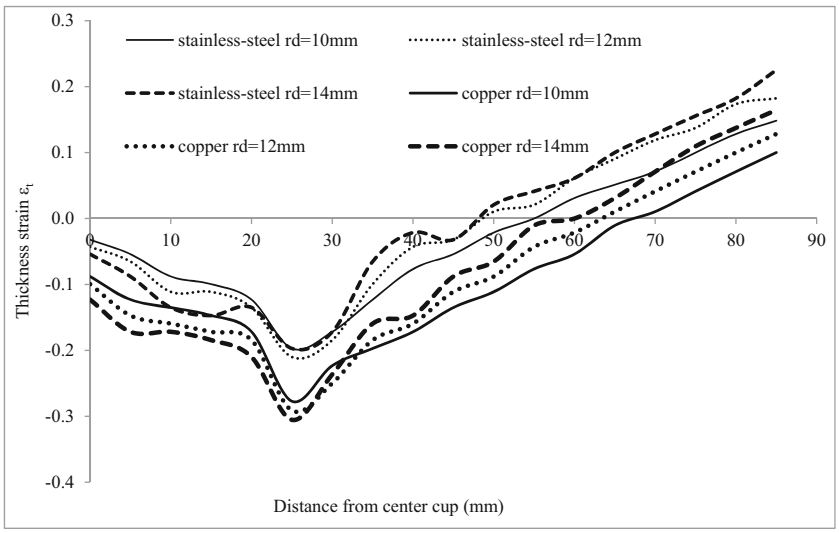

Fig. 10 Thickness strain distributions of SUS 304L and copper layers of drawn clad cup for different r_d, DR=2.3, $r_P=5t_0$, BHP=0.875 MPa, friction state=Oil+Pe, RD

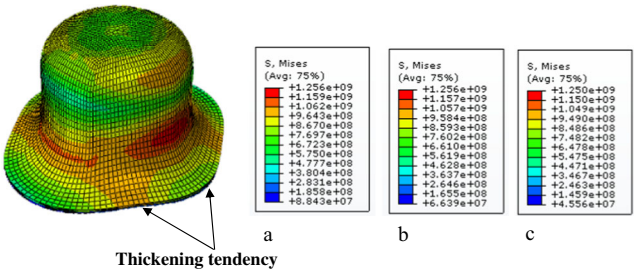

Fig. 11 Distribution of forming stresses for different r_d, **a** $r_d=5t_0$; **b** $r_d=6t_0$; **c** $r_d=7t_0$ DR=2.3, $r_P=5t_0$, BHP=0.875 MPa, friction state=Oil+Pe

region. For the copper-stainless-steel 304L clad cups, valleys are created in DD and ears in RD; as a result, in RD the cup wall is thinner but longer in height.

Anisotropy coefficients for the single-layer copper sheet in Table 3 and Figs. 13 and 14 reveal that the single-layer copper sheet behaves approximately isotropic and the thickness in different directions is the same; besides, for the single-layer stainless-steel 304L sheet cup wall in RD is thicker than DD.

Figures 13 and 14 show that the discrepancy between the peaks, maximum and minimum thickness distributions of the clad sheet is higher than that of the single-layer sheets. This phenomenon is attributed to the materials of the clad sheet that the planar anisotropic properties are higher than the single-layer sheet mainly due to cold-work history and post-heat treatment leading to an increase between valleys and ears height. Thus, thinning and thickening in the clad cup are elevated.

Comparison of the thickness distributions for the same layer set in the external and/ or internal layers as shown in Figs. 13 and 14 indicates that as the elements of the external layer in comparison to the internal layer that are under more extension, due to bending and drawing at the punch nose, make this layer thinner and its behavior more similar to the same single-layer sheets. Moreover, non-uniform distribution of thickness strain is more pronounced where the copper is at the outside of the deformed clad cup.

It is noteworthy that the sheet-set condition has a significant influence on the thickness strain behaviors of the deformed clad cup. When the inside layer of the drawn clad sheet is relatively stronger, the summation thickness of the clad cup decreases, compared to the reversed sheet-set condition. When the strong layer is located inside of the drawn clad sheet, the tensile stress which is higher at the outer layer (the weak layer), hence its thickness decreases; thus, the thickness of the overall clad sheet decreases too.

4.5.2 Comparison of the forming stresses for internal and external layers

The internal and external layers behavior of the clad sheet is analyzed using the von Mises stress distribution by the FE simulation (Fig. 15). In this analysis, it is shown that plastic deformation initially occurs in the copper layer. This layer is then undergone further deformation with almost a constant stress (close to the ultimate tensile strength of material) without any fluctuation. For stainless-steel layer, variations in stresses are negligible at the bottom and corner radius of the cup while in the cup wall the higher stresses appear depending on the element positions, due to earing. Higher stresses are flowed to the elements that undergone higher strains. These higher stresses in stainless-steel are related to work-hardening exponent of this material. In addition, the von Mises stresses are higher at valleys due to normal anisotropy of materials, r value, in direction of 45° is higher than two other directions 0° and 90°. A high r value causes high deformation resistance of blank (the thicker portions require more stress for forming). It is worth mentioning that the forming

Fig. 12 The Effects of BHP on clad and single-layer cups for DR=2.3, $r_d=r_p=5t_0$, friction state=Oil+Pe, **a** BHP=0.875–4 MPa; **b** BHP=8–10 MPa

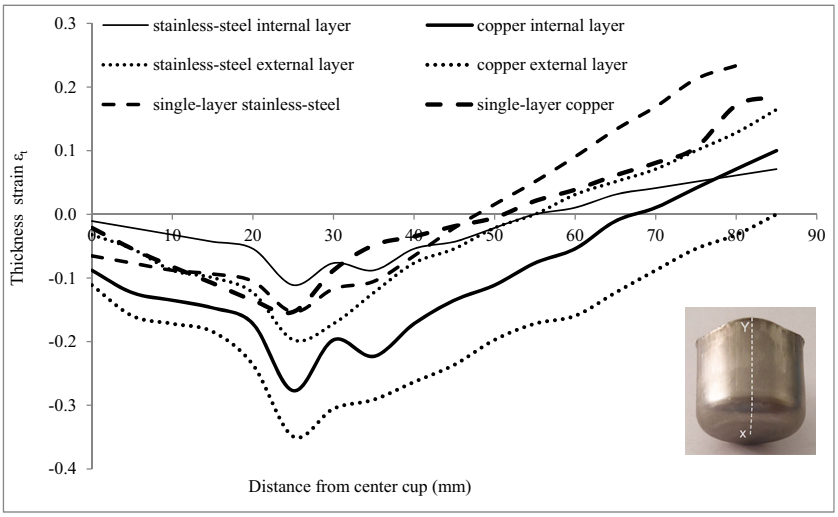

Fig. 13 Thickness strain distributions of SUS 304L and copper layers of drawn clad and single-layer cups, DR=2.3, r_d=r_P=5t_0, BHP=0.875 MPa, friction state=Oil+Pe, RD

stresses of the copper where it is located at the external position (in contact with the die) are slightly smaller than the stresses of the internal layer.

The forming stresses are given in Fig. 15 which shows inhomogeneous plastic deformations. This is mainly due to the difference of the tensile strength of stainless-steel material which is about 4.4 times of copper. According to this figure, the copper layer plastic deformation occurred at the beginning of the process, hence it is concluded that the deformation of the clad sheet is controlled by the stainless-steel layer.

4.6 Fracture position prediction

If the blank diameter is larger than that of the critical diameter, axial stresses along the cup wall exceed the tensile strength of the materials and rupture will occur before the process is completed. From the aforementioned results, it can be inferred that the draw ratio for the clad sheet and single-layer one is about 2.3. Hence, for determining the fracture position, FE simulation is carried out considering draw ratio of DR=2.4, r_d=r_p=5 t_0, lubricating state, and BHP=0.875 MPa. In Fig. 16, the strain distributions with respect to the die displacement are given. At the beginning of the process, for die displacement (u) of less than 25.41 mm, as it is shown in Fig. 16a, the strain distributions are uniform and the fracture bands do not appear at this depth. For further die displacement, the strain distributions close to the region having contact with the punch corner radius become non-uniform, as shown in Fig. 16b for u= 28.95 mm. By continuing the process, the strains tending to create small cracks in the work-piece

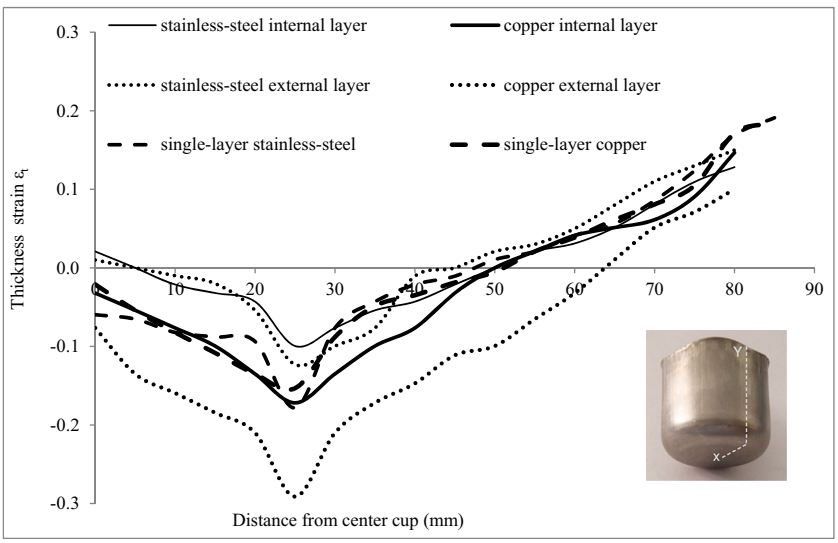

Fig. 14 Thickness strain distributions of SUS 304L and copper layers of drawn clad and single-layer cups, DR=2.3, r_d=r_P=5t_0, BHP=0.875 MPa, friction state=Oil+Pe, DD

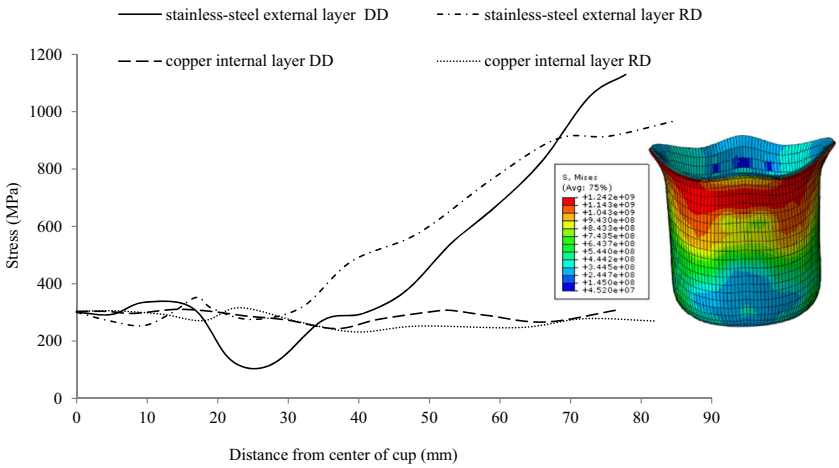

Fig. 15 Forming stress profiles of SUS 304L and copper layers in deformed clad cup, DR=2.3, RD and DD r_d=r_P=5t_0, BHP= 0.875 MPa, friction state=Oil+Pe

developed in the circumferential region of the cup. The values of the major logarithm strains in both layers reach the critical value and bring about fracture at the cup corner as shown in Fig. 16c. Figure 17a, b exhibits a comparison between the fracture occurring in experiment and the FE simulation. Fracture was observed for

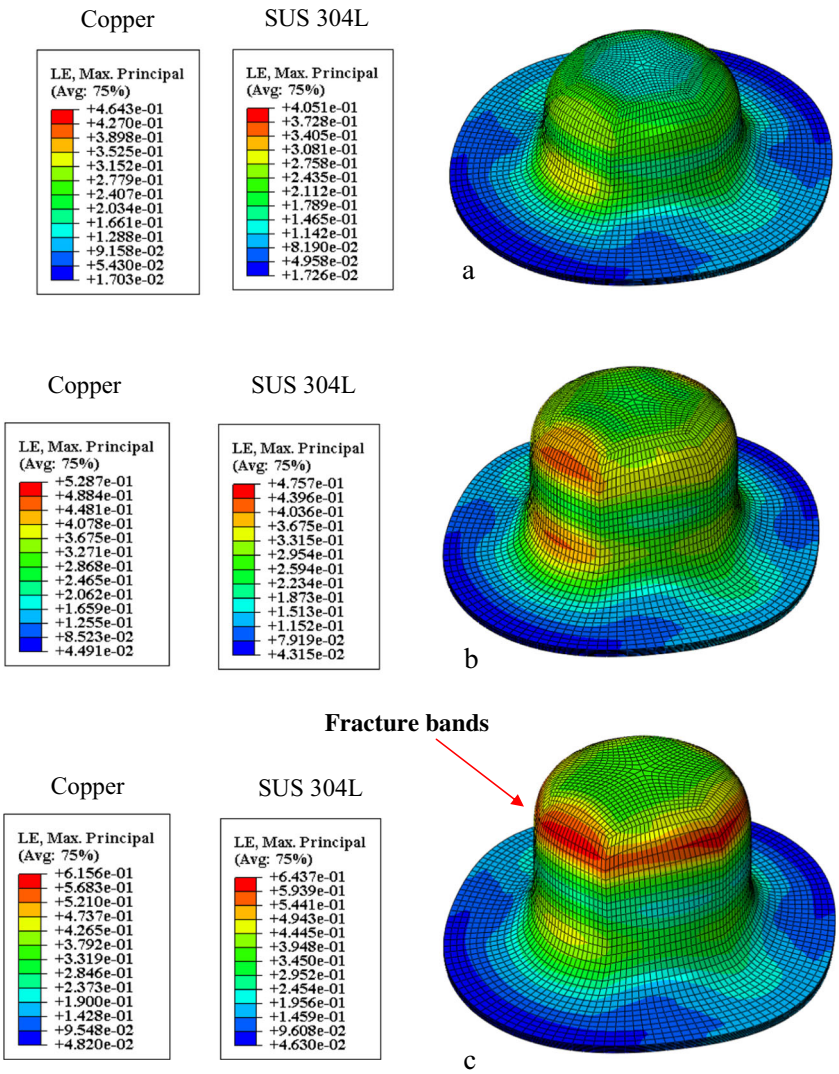

Fig. 16 Distributions of major logarithm strain for different die displacements **a** u=25.41 mm, **b** u=28.95 mm, and **c** u=30.63 mm

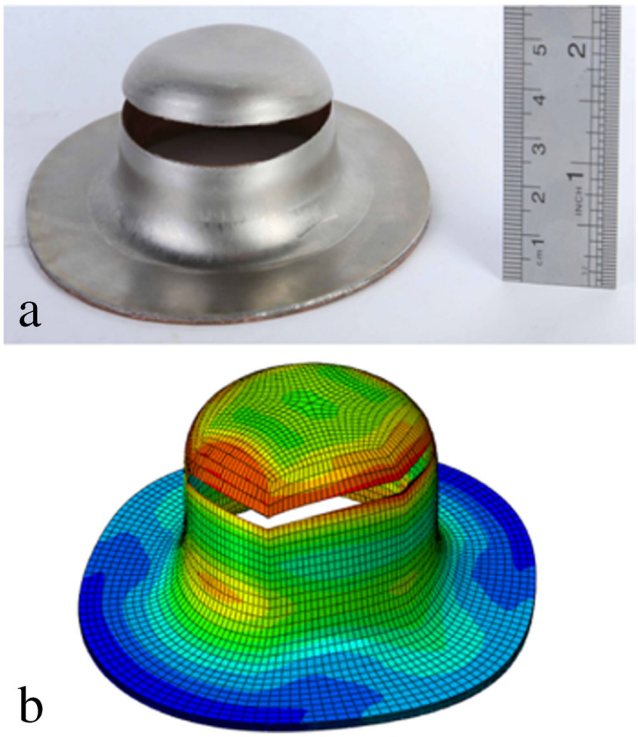

Fig. 17 **a** experimental and **b** FE simulation of fracture positions for DR=2.4

die displacements of u=29.75 mm and u=30.63 mm in the experimental tests and FE simulations respectively, which are both in good agreements.

As it is seen, tear does not occur in clad cup at the cup bottom on account of high work-hardening exponent and average r values in the components metal of clad sheet. Fracture only occurred on the cup corner that is inevitable for high-draw ratios.

According to Fig. 16c, the strain of the elements in the external layer, stainless-steel, is a little bit closer to the necking line compared to those of the internal layer, copper. This is related to stainless-steel material strength which is higher than that of the copper. Hence, the logarithm strain is more pronounced in this layer.

Similar results were observed for single-layer stainless-steel 304L cups and single-layer copper cups for die displacements of u=31.23 mm and u=28.8 mm respectively.

5 Conclusions

The main objective of this research was to study the formability of clad sheet of copper stainless-steel. Experimental tests were carried out to determine the effective parameters of the process. According to the experiments, when clad sheets were heat-treated in a similar condition that formability for the single-layer sheets emerged, the diverse layout setting had no influence on the drawability of the clad metal sheet. The following remarks can be obtained from this study:

(1) The limiting draw ratio for clad and single-layer sheets was 2.3 and in deep drawing of copper stainless-steel-clad sheets the suitable conditions were found to be $5t_0$ for die and punch edge radius, oil and polyethylene as lubricant and a blank holder pressure of 0.875 MPa.
(2) Thickness distribution measurement in different rolling directions indicated that the thickness of clad cups in the RD was less than that of DD. In contrast, the thickness distributions in the single-layer copper in different rolling directions is approximately the same and the thickness of the single-layer stainless-steel 304L sheet cup wall in RD is thicker than DD.
(3) The difference between r value in the clad sheet in both layers was higher than that of the single-layer sheets leading to discrepancies between the maximum and minimum thickness distributions in the clad sheet which is higher than that of the single-layer sheet.
(4) Comparison of the thickness variations for the same layer set in the internal and/ or external layer illustrated that the thickness of the external layer reduced more in comparison to that of the internal layer.
(5) The thickness distribution of stainless-steel 304L (stronger layer) was somewhat more uniform than the weaker (copper) one.
(6) The FE simulation of the clad sheet showed that the layer with a higher strength was exposed to higher stresses as expected and deformation in deep drawing was controlled by the stronger (stainless-steel) layer.
(7) From the FE simulation and experiment results, fracture occurred at the top corner cup if the strains exceed the critical strain. The strains of the elements at the external layer were a bit closer to the necking line than the internal elements.

References

1. Li L, Nagai K, Yin F (2008) Progress in cold roll bonding of metals. Sci Technol Adv Mater 9:023001
2. Danesh Manesh H, Shahabi HS (2009) Effective parameters on bonding strength of roll bonded Al/St/Al multilayer. J Alloys Compd 476:292–299
3. Lee JE, Bae DH, Chung WS, Kim KH, Lee JH, Cho YR (2007) Effects of annealing on the mechanical and interface properties of stainless steel/aluminum/copper clad-metal sheets. J Mater Process Tech 187–188: 546–549
4. Bina MH, Dehghani F, Salimi M (2013) Effect of heat treatment on bonding interface in explosive welded copper/stainless steel. Mater Des 45:504–509

5. Danesh Manesh H, Karimi Taheri A (2003) Bond strength and formability of an aluminum-clad steel sheet. J Alloys Compd 361: 138–143
6. Sheng LY, Yang F, Xi TF, Lai C, Ye HQ (2011) Influence of heat treatment on interface of Cu/Al bimetal composite fabricated by cold rolling. Compos Part B-Eng 42:1468–1473
7. Verma RK, Chandra S (2006) An improved model for predicting limiting drawing ratio. J Mater Process Tech 172:218–224
8. Yang TS (2008) The application of abductive networks and FEM to predict the limiting drawing ratio in sheet metal forming processes. Int J Adv Manuf Technol 37:58–69
9. Ozek C, Bal M (2009) The effect of die/blank holder and punch radiuses on limit drawing ratio in angular deep-drawing dies. Int J Adv Manuf Technol 40:1077–1083
10. Chen FK, Lin SY (2007) A formability index for the deep drawing of stainless steel rectangular cups. Int J Adv Manuf Technol 34: 878–888
11. Savas V, Secgin O (2007) A new type of deep drawing die design and experimental results. Mater Des 28:1330–1333
12. Browne MT, Hillery MT (2003) Optimising the variables when deep-drawing C.R.1 cups. J Mater Process Technol 136:64–71
13. Colgan M, Monaghan J (2003) Deep drawing process: analysis and experiment. J Mater Process Technol 132:35–41
14. Gavas M, Izciler M (2006) Deep drawing with anti-lock braking system (ABS). Mech Mach Theory 41:1467–1476
15. Rees DWA, Power RK (1994) Forming limits in a clad steel. J Mater Process Technol 45:571–575
16. Hino R, Yoshida F, Okada T (1998) Deep drawability of sheet metal laminates. J S M E A 64(621):1397–1403
17. Habibi Parsa M, Yamaguchi K, Takakura N (2001) Redrawing analysis of aluminum–stainless-steel laminated sheet using FEM simulations and experiments. Int J Mech Sci 43:2331–2347
18. Youshida F, Hino R (1997) Forming limit of stainless steel-clad aluminium sheets under plane stress condition. J Mater Process Technol 63:66–71
19. Tseng HC, Hung C, Hung C, Huang CC (2009) An analysis of the formability of aluminum/copper clad metals with different thicknesses by the finite element method and experiment. Int J Adv Manuf Technol 49:1029–1036
20. Chen C, Kuo J, Chen H, Hwang W (2006) Experimental investigation on earing behavior of aluminum/copper bimetal sheet. Mater Trans JIM 47:2434–2443
21. Padmanabhana R, Oliveira MC, Alves JL, Menezes LF (2007) Influence of process parameters on the deep drawing of stainless steel. Finite Elem Anal Des 43:1062–1067
22. Akamatsu T, Ukita S, Miyasaka K, Shi M (1995) Deep drawing of commercially pure titanium sheets. ISIJ Int 35:56–62
23. Ibrahim D, Esner H, Yasar CM (2008) Effect of the blank holder force on drawing of aluminum alloy square cup: theoretical and experimental investigation. J Mater Process Technol 206:152–160
24. Mori T, Kurimuto S (1996) Press-formability of stainless steel and aluminum clad sheet. J Mater Process Technol 56:242–253
25. Takuda Mori HK, Fujimoto H, Hatta N (1996) Prediction of forming limit in deep drawing of Fe/Al laminated composite sheets using ductile fracture criterion. J Mater Process Technol 60:291–296
26. Takuda H, Hatta N (1998) Numerical analysis of the formability of an aluminum 2024 alloy sheet and its laminates with steel sheets metal. Mater Trans A 29:2829–2834
27. Atrian A, Fereshteh-Saniee F (2013) Deep drawing process of steel/brass laminated sheets. Compos Part B 47:75–81